ground water

Conventional and Combined Pump-and-Treat Systems Under Nonuniform Background Flow

by Peter Bayer[1] and Michael Finkel[2]

Abstract

We investigate the performance of vertical hydraulic barriers in combination with extraction wells for the partial hydraulic isolation of contaminated aquifer areas. The potential advantage of such combinations compared to a conventional pump-and-treat system has already been demonstrated in a previous study. Here we extend the scope of the performance analysis to the impact of uncertainty in the regional flow direction as well as to highly heterogeneous aquifer transmissivity distributions. In addition, two new well-barrier scenarios are proposed and analyzed. The hydraulic efficiency of the scenarios is rated based on the expected (mean) reduction of the pumping rate that is required to achieve downgradient contaminant capture. The uncertain spatial distribution of aquifer transmissivity is considered by means of unconditioned Monte Carlo simulations. The significance of uncertain background flow conditions is incorporated by computing minimized pumping rates for deviations of the regional flow direction up to 30° from a normative base case. The results give an answer on how pumping rates have to be changed for each barrier-well combination in order to achieve robust systems. It is exposed that in comparison to installing exclusively wells, the barrier-supported approach generally yields savings in the (average) pumping rate. The particular efficiency is shown to be highly dependent on the interaction of variance and integral scale of transmissivity distribution, well and barrier position, as well as direction of background flow.

Introduction

Once penetrated into an aquifer, pollutants such as organic chemicals can stay for decades as sources for contaminant plumes in ground water. This is especially true for sites that are contaminated with dense non–aqueous phase liquids (DNAPLs), which form a separate phase in the subsurface posing a big challenge to planners and decision makers. So far, even aggressive remediation technologies failed to achieve total clean up at these sites. The U.S. EPA (2003) reports that "there is no documented, peer-reviewed case study of DNAPL source-zone depletion beneath the water table where U.S. drinking water standards or MCLs (maximum contaminant levels) have been achieved and sustained throughout the affected subsurface volume, regardless of the in-situ technology applied." Therefore, in most cases, long-term control measures are required that ensure that contaminants do not migrate off-site. Since sites where natural attenuation processes are effective enough to meet the remedial objective are rather the exception than the rule, in most cases, engineered measures are required to guarantee appropriate control of the contaminants in ground water, i.e., to prevent damage to the adjacent environment.

A common approach is to hydraulically isolate the contamination. This can be achieved by several different technologies. Most common are extraction wells positioned inside or downgradient of a contamination. By continuous pumping, capture zones are created covering the contained aquifer. The extracted ground water usually has to be cleaned up, entailing high operational costs for pumping and treatment. Obviously, this is of major economic concern if the pump-and-treat system (PT) is intended to provide long-term control and needs to be operated for years

[1]Corresponding author: Center for Applied Geoscience, University of Tuebingen, Sigwartstrasse 10, 72076 Tuebingen, Germany; (49) 7071-2973178; fax (49) 7071-5059; peter.bayer@uni-tuebingen.de

[2]Center for Applied Geoscience, University of Tuebingen, Sigwartstrasse 10, 72076 Tuebingen, Germany; (49) 7071-2973177; fax (49) 7071-5059; michael.finkel@uni-tuebingen.de

Received November 2004, accepted April 2005.

doi: 10.1111/j.1745-6584.2005.00191.x

or even decades. Another option is in situ treatment by completely passive systems such as permeable barriers or biocurtains, with higher installation but expectably lower operational costs (Powell et al. 2002). Practical or economic considerations may militate in favor of hybrid approaches representing combinations of different technologies. As an alternative to using exclusively pumping wells, among others, Cunningham and Reinhard (2002) discuss hydraulic control by the use of injection-extraction treatment well pairs. They examine their technology with respect to hydraulic efficiency and operating and maintenance costs and discuss situations where this is preferable over a completely passive system. Bayer et al. (2001, 2003a, 2003b, 2004, 2005) go a similar way for the combination of pumping wells with vertical hydraulic barriers such as sheet piles or slurry walls. It is revealed that depending on the position of a barrier and economic and physicochemical boundary conditions, these combined PT involving barriers (barrier-supported pump-and-treat systems [BPT]) can be advantageous. Barriers can significantly reduce the pumping rate of extraction wells required to capture the contamination in an aquifer, with highest benefits at high flow rates, high treatment costs, and relatively low barrier installation costs. The perspective of this technology is not to accelerate clean up but to hydraulically control critical aquifer zones over a long time period. It is obvious that changes in flow regime and contaminant mass transfer rates into the passing ground water affect the cleanup progress. However, it is assumed that, similar to the application of permeable barriers, short-term remediation is either not possible or merely not planned. Bayer et al. (2005) demonstrate that solely from an economical point of view, due to commonly expectable interest returns, the influence of the operation time on net present expenditures is only marginal for measures planned over decades.

The presented study is the sequel to a preceding paper (Bayer et al. 2004) that dissects the hydraulic characteristics of a number of BPT scenarios assuming homogeneous and moderately heterogeneous transmissivity distribution. Here, we extend the number of these scenarios characterized by the relative position of the contaminated source and vertical barrier(s). Furthermore, it is illustrated how the performance of BPT compared to conventional pump-and-treat systems (CPT) changes at high heterogeneity levels. For this, unconditional Monte Carlo simulations are used assuming static ground water flow conditions. Natural aquifers, however, are dynamic systems with fluctuations in the flow system. Records of the ground water surface or the potentiometric head typically show variations in the regional flow direction, with seasonal changes in hydraulic gradient controlled by shifting seepage levels in open water bodies, rainfall, or anthropogenic activity (e.g., Serfes 1991; Erskine 1991). It is obvious that gradient variations are particularly important in determining the overall success of hydraulic measures. So far, however, the main focus in the research of capture zone delineation is set on uncertainty in physical aquifer parameters such as conductivity and porosity (e.g., Bair et al. 1991; Pranzetti and Guadagnini 1996; Cole and Silliman 1997; van Leeuwen et al. 2000; Zhang and Lu 2004; Feyen et al. 2004). Zawadzki et al. (2002) show that for PT design, one should especially account for these gradient variations when the period of fluctuations in the hydraulic gradient approaches the travel time of the contaminant. Jacobson et al. (2002) analyze the form of capture zones under transient flow and cyclic gradient variations by an analytic approach. Reilly and Pollock (1996) as well as Festger and Walter (2002) use forward particle tracking to estimate the average ratio of particles captured at changing regional flow direction, which Festger and Walter (2002) illustrate by capture efficiency maps. In the presented work, we focus on the relevance, i.e., the hydraulic effect of deviations in the flow direction from a given (expected) direction on PT performance. This means that we do not analyze the transient effect of the gradient fluctuations but consider the envelope of these fluctuations by using a steady-state approach and by modeling ultimate capture zones. It is implicitly presumed that a principal uncertainty exists in the regional flow direction due to measurement errors or insufficient site data. The purpose is to derive robust hydraulic control systems, which can cope with a certain uncertainty in the flow direction.

Methodology

CPT and BPT Scenarios

Equivalent to the approach by Bayer et al. (2004), a hypothetical base-case model is established with a regional flow direction oriented north-south (NS). As shown in Figure 1 for CPT, a quadratic contaminated area is considered that has to be hydraulically captured by a single pumping well positioned downgradient of the area along the centerline. The side length of this area is given by w, and the distance to the downgradient well is x. Cases with $x/w = 0.25$, 0.5, 0.75, and 1.0 have been inspected. For BPT scenarios, hydraulic barriers are added, each of them characterized by a particular position of the barrier(s) relative to the contaminated area. In principle, an endless number of different scenarios could be generated. For the purpose of this study, as we aim at a general investigation

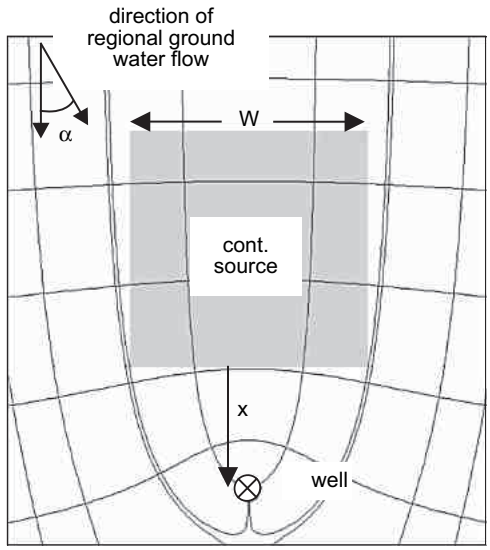

Figure 1. Scheme of CPT with quadratic contamination and downgradient well (horizontally oriented head contour lines, perpendicular pathlines).

of BPT performance, we deliberately limit the range of scenarios to a set of representative pumping well-wall combinations. All scenarios are laterally symmetrical, and barriers are either placed at the edge or center of the contaminated area (Figure 2). The scenarios with one linear barrier each positioned upgradient, downgradient, and in the center of the contaminated zone perpendicular to the flow of the base case are denoted as "up," "down," and "mid." Scenarios "updown" and "side" signify two-barrier cases of walls at the fringe of the contaminated area perpendicular and, respectively, longitudinal to the regional flow. The "upside" scenario has one wall at the upgradient edge of the contamination and two at the sides. The total barrier length for each scenario is denoted as b and measured in multiples of w. In the subsequent analysis, unless otherwise stated, we focus on selected variants of the BPT scenarios with fixed barrier lengths as shown in Figure 2 (scenarios up, down, and mid: $b/w = 1$, scenarios updown and side: $b/w = 2$, scenario upside: $b/w = 3$).

Model Setup and Evaluation Procedure

For the modeling of ground water flow and hydraulic effects of the CPT and BPT scenarios, we used the USGS finite-difference model MODFLOW (McDonald and Harbaugh 1988). Ground water flow is assumed to be confined and steady state and is described in two dimensions. The flow domain is discretized by 300×300 quadratic cells of 1-m side length each. A regional gradient $i_{\text{region}} = 0.001$ is imposed by fixed head boundaries around the model domain. Deviations of the flow direction from the base case (NS orientation, deviation angle $\alpha = 0°$) are considered at 5° steps anticlockwise up to 30° (deviation angle $\alpha = 0°$ to 30°) by changing the heads at the model boundaries. A 50- × 50-m contaminated area is positioned in the middle of the model with its downgradient edge in the center of the model. The capture performance of any particular scenario at given settings of b/w, x/w and α is evaluated by means of an advective control approach using the particle-tracking routine MODPATH (Pollock 1994). To do this, the edge of the contaminated area is delineated by 200 uniformly distributed particles. These particles are tracked forward along the flow lines, recording whether a particle ends up in the "well cell" (specified as distributed sink that captures particles only if it is representing a strong sink) or not.

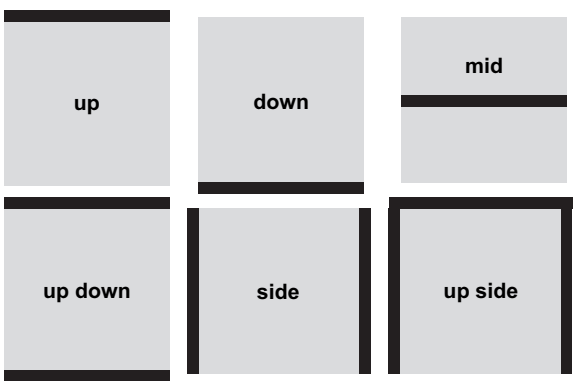

Figure 2. Relative position of barriers (black lines) for BPT scenarios to quadratic contamination (gray).

The objective is to minimize the pumping rate of the well based on the assumption that operational costs are directly correlated to the pumping rate. The minimum pumping rate is computed iteratively by the bisection method of Press et al. (1992) using an external solver. The simulation model was run up to 15 times to obtain a solution at a relative precision of >99%. An optimized system captures all particles (entirely contains the contaminated area) at a minimum pumping rate. To simplify matters, it is assumed that no contaminant plume evolved before the start of the PT measure and thus would have to be additionally captured.

Both homogeneous and heterogeneous aquifer conditions were examined. A hydraulic transmissivity, $T = 0.01$ m^2/s, was used for the homogeneous case and as a log mean value for the heterogeneous case. For heterogeneous aquifer conditions, we further assume that only statistical properties of the spatial transmissivity distribution are known. Uncertain knowledge about the transmissivity field is represented by sets of 500 aquifer realizations randomly produced by unconditional sequential Gaussian simulation (SGS; Deutsch and Journel 1992). Using SGS, the anisotropic spatial transmissivity distribution can be modeled by defining only three parameters. Each set of 500 realizations is characterized by a given variance, σ_Y^2, of the lognormal distributed isotropic transmissivity, T, its log mean, and an integral scale, I_Y, which denotes the spatial continuity of the probability distribution function Y. Assuming, in this study, that there is a linear relationship between calculated pumping rates and log mean transmissivity, variable parameter combinations of σ_Y^2 and I_Y can be defined to cover a broad range of statistically different spatial transmissivity structures. Like other linear dimensions, the integral scale is also normalized with respect to the width, w, of the contaminated area. The realizations of the presented study are computed with values of $I_Y/w = 0.25$, 0.5, and 1.0 and $\sigma_Y^2 = 0.1$, 0.5, 1.0, 2.0, 3.0, and 4.5.

Though one of the most common methods, SGS is only one of many options to stochastically model transmissivity distributions of aquifers. There are many alternative approaches available including fractal-based models (Molz et al. 2004) or hydrofacies-oriented simulations (Carle and Fogg 1996; Maji et al. 2005). Comparative studies exhibit specific features of geostatistical simulation algorithms (e.g., Gotway and Rutherford 1994; Gomez-Hernandez and Wen 1998; Zinn and Harvey 2003, Lemke et al. 2004), but as Goovaerts (1999) states, "it seems unlikely that the entire set of possible outcomes could be sampled by a single class of algorithms." When comparing conditioned SGS with alternative approaches, he comes to the conclusion that SGS is preferable due to large goodness statistics as well as small local uncertainty. Wen and Gomez-Hernandez (1998) emphasize the inability of multivariate Gaussian models such as SGS to simulate continuity of extreme values and instead recommend nonparametric approaches such as sequential indicator simulation. Since the occurrence of a high-conductivity channel plays an important role in contaminant transport, this aspect will be discussed further when looking at the modeling results.

After creating the transmissivity maps by SGS, system optimization, i.e., the minimization of the pumping rate, was performed individually for each realization. All minimized pumping rates of each ensemble of 500 realizations were then sorted for each setting of CPT and BPT in order to obtain a cumulative density function (cdf) of "success." The cdf depicts the relationship between pumping rate and the proportion of realizations for which capture is achieved. If a fixed well position is considered, the cdf steadily increases with the pumping rate. We also evaluate realization-specific differences in Q' for CPT compared to BPT scenarios. The cdfs of these differences characterize the probability of savings in required pumping rate by the use of barriers (cf., Bayer et al. 2004). Here, a condensed illustration of the results is presented and mainly average savings are discussed. However, even if savings can be anticipated on the average, the question remains, how big is the probability that barriers lead to a deterioration compared with using wells exclusively? Therefore, the frequency of realizations with worse results for BPT scenarios than for CPT is additionally scrutinized.

Please note that minimized pumping rates are expressed as dimensionless values, Q'. This was done by normalization of modeled pumping rates Q to the undisturbed uniform flow rate through the contaminated area at homogeneous conditions:

$$Q' = \frac{Q}{Ti_{\text{region}} w} \tag{1}$$

This way, generally valid results are obtained that are independent from the actual flow model used. As an illustration, consider the homogeneous base case: a pumping well positioned centrally at the downgradient edge without any barriers has to pump twice the undisturbed flow rate ($Q' = 2$) to fully capture the contaminated area. At a distance of $x = w/2$, Q' reduces to 1.38 and at $x = w$, to $Q' = 1.21$ (Bayer et al. 2003b). At increasing distances, Q' asymptotically approximates 1 but can never go below this value. For heterogeneous aquifers, the presumed statistics on spatial transmissivity distributions are expected to reflect those of real sites at the same scale. For a more detailed discussion on hydrogeologic scaling, the reader is referred to Schulze-Makuch et al. (1999) and Neuman and Di Federico (2003). The emphasis of this generic model study is to inspect the influence of a predetermined degree of heterogeneity on BPT compared to CPT. To obtain general site-unspecific results, unconditional SGS was used, which does not account for point measurements given at a real site such as conditional simulations. It is evident that a more detailed picture of the transmissivity distribution calls for a site-specific adaptation of hydraulic measures, which is not analyzed further in this study.

Implications of Previous Findings

In our precursory study (Bayer et al. 2004), the up, down, updown, and upside scenarios were inspected in terms of their performance under homogeneous and moderate heterogeneous flow conditions. No deviations of the flow direction from the NS orientation were assumed. For homogeneous aquifers, it was illustrated how ideal barrier positions change depending on the given total barrier length. Downgradient barriers are preferable if the barrier length is lower than or equal to the width of the contaminated area. Increasing the barrier length favors the updown scenario, and, at b/w close to 3, the upside scenario leads to the lowest pumping rates. The influence of heterogeneous transmissivity distributions was inspected for a selection of specific BPT scenarios with fixed barrier lengths b/w (same lengths as illustrated in Figure 2). Statistical properties of the transmissivity field were oriented at characteristics of the Borden site ($\sigma_Y^2 \leq 1.8$ and integral scales I_Y/w between 0.18 and 1.8). It was shown that the mean and variance of the calculated pumping rates for ensembles of 500 equally probable realizations increase with both σ_Y^2 and I_Y/w. In general, absolute BPT savings also increase and the probability that barriers lead to worse results than CPT was close to zero. It was further revealed that the pumping rate distributions for the BPT scenarios considered have a lower variance than those of CPT, indicating a higher robustness of hydraulic systems with barriers than of wells alone.

Results of Hydraulic Analysis

Gradient Variation for Homogeneous Aquifers

The calculations assuming a homogeneous spatial transmissivity distribution provide some elementary insights into the effect of barriers on pumping rates Q' required for capture of the contaminant area. The barrier lengths of the BPT scenarios chosen are set fixed here according to the schemes depicted in Figure 2, at $b/w = 1$ for the single-barrier scenarios (up, down, mid), $b/w = 2$ for two barriers (side, updown), and $b/w = 3$ for the angular configuration (upside). As shown in Figure 3, the values of Q' for the BPT scenarios are below those for CPT. Scenarios with high barrier lengths, such as the scenarios updown and upside, are most significantly decreasing Q', with rates below the Darcy flow rate through the contaminated zone ($Q' < 1$). Barriers at the lateral sides alone rarely hinder the flow through the contamination and therefore lead to comparatively higher Q', similar to those of single-barrier configurations. The most favorable single-barrier BPT turns out to be the one with downgradient position, particularly proficient at a low distance of the well $x/w = 0.25$ (Figure 3a). Increasing this distance lowers Q' for all scenarios and simultaneously reduces the relative savings that can be achieved by the installation of barriers. The pumping rates of the single-barrier scenarios differ only slightly at $x/w = 1.0$ (Figure 3b).

Changing the gradient direction by angle α has a distinct influence on the BPT systems considered. Due to the deviation of the flow orientation from NS, the values of Q' increase for all scenarios, with higher rates at higher well distances. As can be observed for most scenarios in Figure 3, there is no exact linear relationship between the values of α and Q'. Generally, changes of α have the

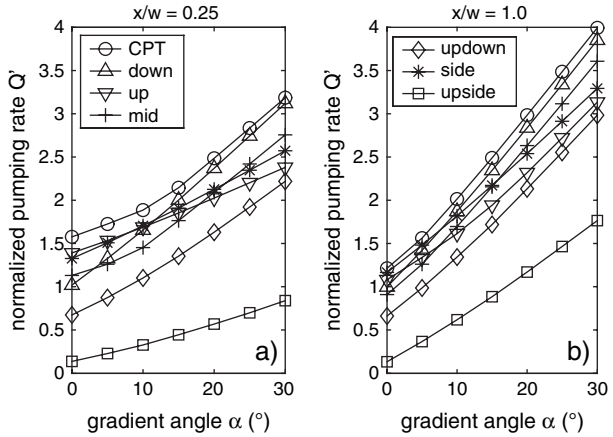

Figure 3. Relationship between minimized dimensionless pumping rate Q' and deviation of the gradient direction from NS. Results for CPT and BPT scenarios for homogeneous aquifer for downgradient well distance of $x/w = 0.25$ and $x/w = 1.0$.

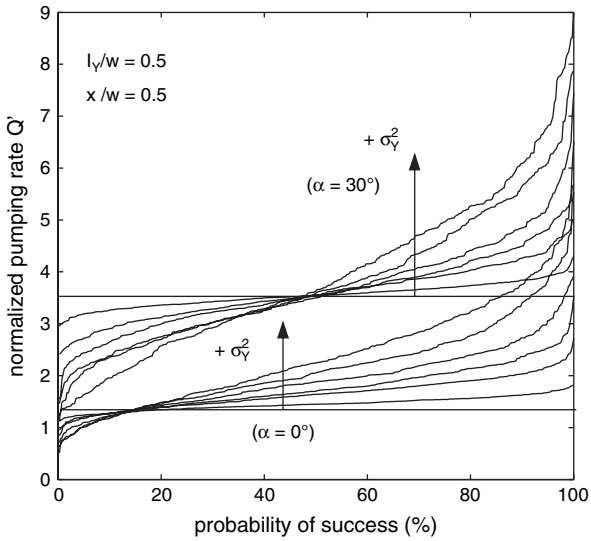

Figure 4. Probability of capture for given normalized pumping rates of CPT at fixed position of well ($x/w = 0.5$) and constant integral scale of hydraulic transmissivity distribution ($I_Y/w = 0.5$). The arrows show the cdfs of increasing variance $\sigma_Y^2 = 0.1, 0.5, 1.0, 2.0, 3.0$, and 4.5.

lowest influence on Q' at low values of α. A striking feature is the specific sensitivity of the selected BPT scenarios on varying the gradient angle. The pumping rates for the updown and mid scenarios rise similar to the results for CPT. There is a minor sensitivity of the scenarios side and upside, indicating that NS-oriented barriers extenuate the influence of gradient variation. This way, the lateral extension of the contamination is obstructed. Obviously, this effect can also be achieved by an upgradient barrier position, which increasingly outperforms the other single-barrier systems.

Gradient Variation for Heterogeneous Aquifers

For a first inspection, the barrier lengths are held fixed according to the settings of the homogeneous case (cf., Figure 2). Also, the well position is not varied ($x/w = 0.5$), and only the variance, σ_Y^2, of the spatial transmissivity distribution is changed (integral scale of half the width of the contaminated area: $I_Y = w/2$). Figure 4 gives the cdfs of Q' for CPT. Apparently, raising σ_Y^2 yields an increase of the spreading of the calculated pumping rates. The cdfs steepen, denoting an incline of the values of Q' required to attain a certain probability of success. For NS orientation of the regional gradient, the values of Q' at heterogeneous conditions are mostly higher than those derived for the homogeneous aquifer (given the same mean transmissivity and $\sigma_Y^2 = 0$).

A gradient angle of $\alpha = 30°$ elevates the cdfs and causes a slightly more pronounced spreading. However, compared to the pumping rates at homogeneous conditions, an approximately equal frequency of higher and lower Q' is calculated. As has been observed for all BPT and CPT scenarios, the frequency of realizations with higher values of Q' than for the respective homogeneous case rises when decreasing α. This means that Q' derived for homogeneous conditions here underestimates the average Q' assuming heterogeneous conditions.

Figure 5 depicts the trade-off between the scenario-specific mean of the Q' distribution, $\overline{Q}'$, and the gradient angle α. Similar to the observations for homogeneous conditions, generally the values of $\overline{Q}'$ are least sensitive to small angles. As shown, the trade-off curves for different σ_Y^2 rise but also converge with increasing α for all scenarios, indicating a reducing influence of aquifer heterogeneity on the required pumping rate. This is least

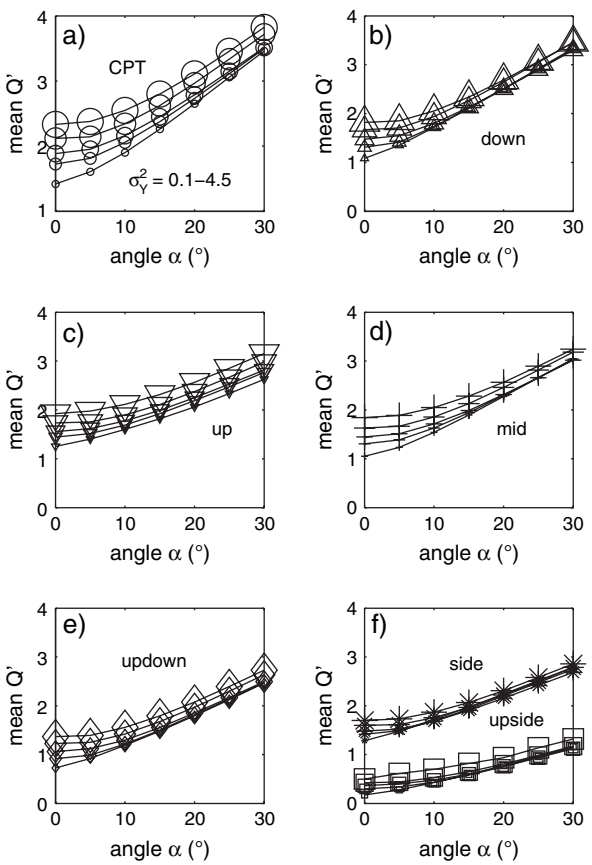

Figure 5. Average values of normalized pumping rates $\overline{Q}'$ for CPT and BPT scenarios for increasing variance (denoted by increasing marker size, $\sigma_Y^2 = 0.1, 0.5, 1.0, 2.0, 3.0, 4.5$). The integral scale is set fixed to $I_Y = w/2$.

pronounced for the up and updown scenarios. Mean Q' values of the BPT scenarios stay below those calculated for CPT. This is also true when the integral scale I_Y changes. This is exposed in Figure 6 comparing the results for $I_Y/w = 0.25$ and $I_Y/w = 1.0$. Figure 6 also points out that the integral scale may remarkably raise $\overline{Q}'$ if the variance of the transmissivity field is high ($\sigma_Y^2 = 4.5$, Figures 6b and 6d). For $\sigma_Y^2 = 0.1$, the influence of the integral scale is negligible (Figures 6a and 6c). Further inspection of Figure 6 reveals a change of the curves' shape from low to high transmissivity variance. While for $\sigma_Y^2 = 0.1$ the CPT and BPT scenarios' sensitivity to an increased deviation angle is nearly linear (Figures 6a and 6c), the curves' slope increases gradually with α for $\sigma_Y^2 = 4.5$ (Figures 6b and 6d). Here only little adjustment of $\overline{Q}'$ is required at low α values, and the curves' slope at larger α values is generally less than for $\sigma_Y^2 = 0.1$. The upside scenario clearly performs best and is least sensitive to α.

From the discussion of the homogeneous case, we know that the influence of a deviation of the hydraulic gradient from expected regional flow NS direction on Q' rises with the distance of the pumping well (Figure 3). Figure 7 depicts the results of the analysis of the heterogeneous case in terms of mean values $\overline{Q}'$ regarding the same extreme variances as aforementioned, i.e., a nearly homogeneous ($\sigma_Y^2 = 0.1$) and a highly heterogeneous aquifer ($\sigma_Y^2 = 4.5$) at $I_Y = w/2$. Serving as a reference, Figures 7a and 7b show the relationship between distance x/w and $\overline{Q}'$ for a NS-oriented gradient ($\alpha = 0°$). Here no unique relationship between distance x/w and $\overline{Q}'$ can be identified. At low variance, $\overline{Q}'$ decreases with x/w or stays nearly constant (scenarios down, updown, upside). At high variance, the reduction of $\overline{Q}'$ with x/w is less pronounced, and for the upside scenario, $\overline{Q}'$ even increases. For an inclined gradient direction ($\alpha = 30°$, Figures 7c and 7d), we obtain the expected result: raising x/w generally means an increase of $\overline{Q}'$. However, the influence of σ_Y^2 is distinctly less pronounced than for $\alpha = 0°$. Taking the updown scenario as an example, it is revealed that for $\alpha = 30°$, the rise of $\overline{Q}'$, when increasing the variance σ_Y^2 from 0.1 to 4.5, amounts only to ~10%, rather independently of the well distance x/w. For $\alpha = 0°$, we can estimate a 100% rise of $\overline{Q}'$. We attribute this observation to the fact that the directed spreading of the contaminant pathways caused by an inclined gradient direction dominates the undirected spreading due to transmissivity variations. The former steps up the required mean pumping rate to a level that is sufficient to cope with a high transmissivity variance σ_Y^2 without any further remarkable increase in $\overline{Q}'$.

There exist many variants of each of the BPT scenarios illustrated in Figure 2 by changing the barrier length(s) b/w. The influence of the latter on the performance, i.e., the average pumping rate, is shown in Figure 8 for the BPT scenarios up, down, updown, and side. The barriers have been elongated symmetrically from the center, and, for each variant, $\overline{Q}'$ was calculated based on the same realization sets used so far ($\sigma_Y^2 = 0.1$, $\sigma_Y^2 = 4.5$; $I_Y = w/2$). For the updown scenario, both

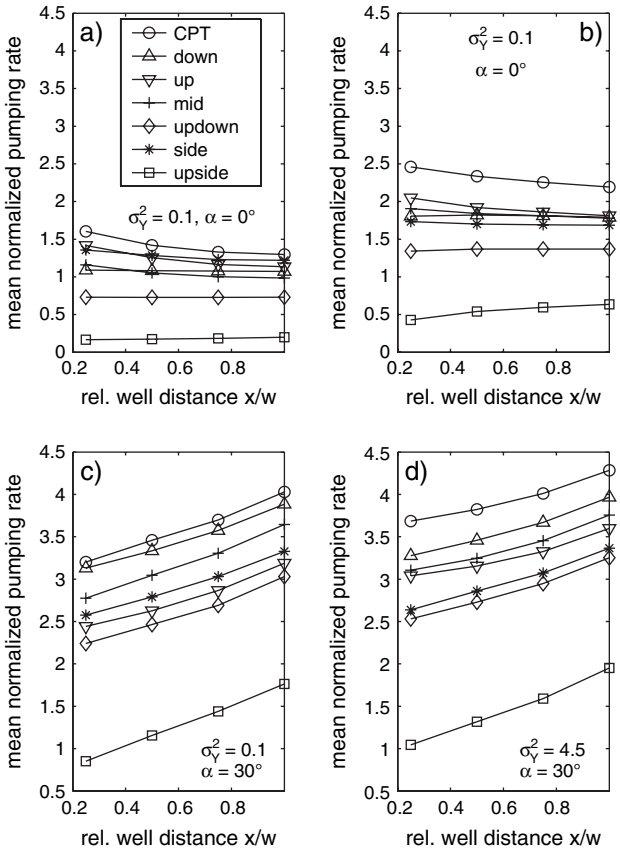

Figure 7. Dependency of $\overline{Q}'$ on relative well distance x/w, for gradient angles 0° and 30°, and variance of transmissivity distribution $\sigma_Y^2 = 0.1$ and $\sigma_Y^2 = 4.5$ (integral scale $I_Y = w/2$).

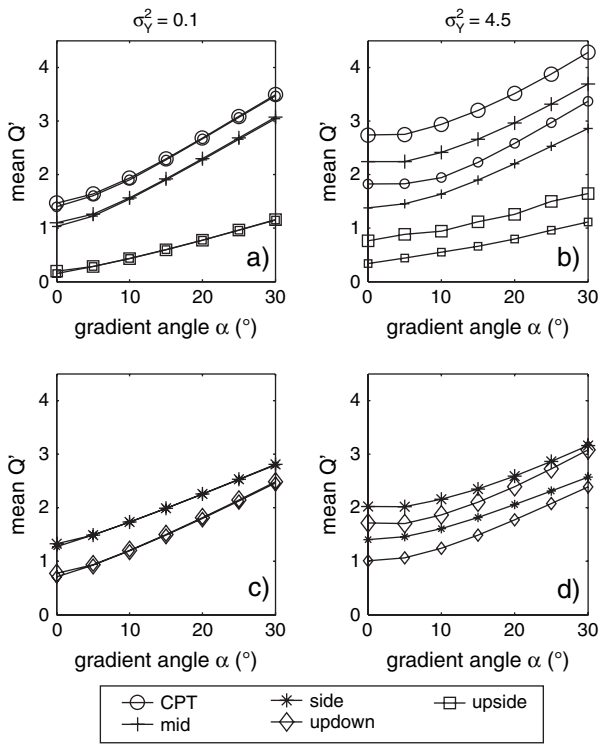

Figure 6. Influence of integral scale I_Y of spatial transmissivity distribution on averaged Q' of CPT and BPT scenarios under different variances $\sigma_Y^2 = 0.1$ (a, c) and $\sigma_Y^2 = 4.5$ (b, d). Small markers represent results for $I_Y = w/4$, large ones delineate $I_Y = w$.

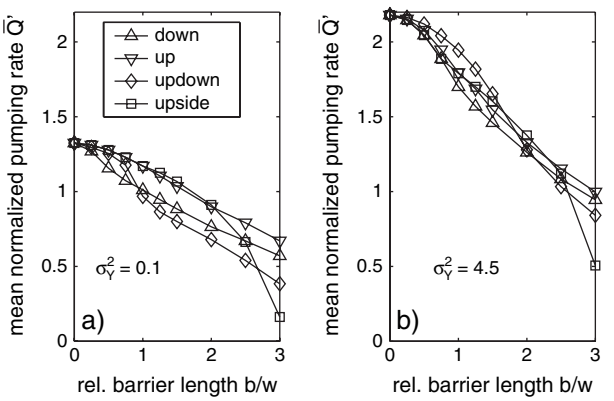

Figure 8. Influence of increasing barrier lengths *b/w* of BPT scenarios down, up, updown, and upside (integral scale $I_Y = w/2$, well distance $x = w/2$). The mean pumping rates $\overline{Q}'$ at $b/w = 0$ represent results for CPT.

barriers have been augmented east-west with the same increments. The variants of the upside scenario have been modified by starting from the upgradient barrier and extending both barriers at the sides to equal portions toward the downgradient direction. For all BPT scenarios, the resulting pumping rates $\overline{Q}'$ decrease at rising b/w, but in detail, there is an individual sensitivity of $\overline{Q}'$ for each particular scenario. At low heterogeneity of the aquifer ($\sigma_Y^2 = 0.1$), over the whole range of $b/w = 0$ to 2.5, the updown scenario gives the best results, which is in accordance with the results under homogeneous flow conditions. Contrary to this, the calculated values of $\overline{Q}'$ for this scenario at high aquifer heterogeneity ($\sigma_Y^2 = 4.5$) are predominantly higher than those of the others. Single-barrier systems are preferable here. At $b/w > 2.5$, independent from the settings for the transmissivity distribution, the most significant effect of a barrier is achieved by the upside scenario. All in all, for the more heterogeneous realization set ($\sigma_Y^2 = 4.5$), a comparably stronger reduction of $\overline{Q}'$ is reached by barrier elongation. This can be attributed to the blocking effect of vertical barriers. Increasing σ_Y^2 raises the discrepancy between high- and low-conductivity zones. As a consequence, contaminant flow focuses in local flow channels. Once cut by transversal barriers, downgradient flow is retained yielding lower contaminant flow rates. These observations are chiefly relevant for site-specific planning of appropriate barrier positions: especially in aquifers with dominant flow channels, an emphasis has to be set on their detection in order to optimize the hydraulic effect of a barrier. From another point of view, natural aquifers with substantial local differences caused by sedimentary facies distributions or fracture patterns seem to be particularly suited for drawing benefits from BPT. For a hypothetical heterogeneous aquifer, Bayer et al. (2001) investigated the hydraulically, as well as economically, ideal barrier position of a BPT with a well positioned in the downgradient vicinity of a contaminant plume. A typical feature was a highly conductive gravel facies oriented in the flow direction in the plume area with most of the contaminant flow concentrated in this zone. It was shown that a barrier, which transversally blocks this channel, is most efficient, yielding the maximum cost savings for this variant. Since there commonly is a significant uncertainty in the description of aquifer hydraulics, existing high-conductivity zones may be imprecisely described or overlooked at real sites. However, their form and orientation is especially crucial for contaminant transport and thus the hydraulic effect of a barrier. The stochastic instead of deterministic modeling approach of this study will reflect the imperfect knowledge of the spatial transmissivity distribution. The question is, what is the preferable barrier position even if we do not know the exact spatial transmissivity distribution, and can savings by installing barriers be expected without their site-specific adaptation? This is inspected in detail in the following section.

Savings by Barriers

In this section, we change the focus and calculate the expected relative savings in Q' that can be reached by installing barriers. Results for an intermediate setting of the model parameters, with $\sigma_Y^2 = 2$, $I_Y = w/2$, and $x = w/2$, are plotted in Figure 9a. A main outcome is that changing the gradient direction leads to different trends in these savings for the individual barrier positions. When α goes up, the BPT scenarios up and side show a percentage increase, whereas for the others, relative savings decline. Especially the opposed responses of the up- and downgradient barrier positions is prominent: their α-savings plots intersect such that the preferable scenario depends on α. An explanation for this observation can be found by comparing the hydraulic effect of these positions. The upgradient barrier insulates the contamination from inflow and yields a convergent flow in the contaminated area. The benefit from the downgradient barrier is the blocking of the outflow, expanding the flow in and out of the contaminated area. This drift is aggravated by an angular flow regime, whereas convergent flow by the upgradient barrier position counters spreading. Consequently, all scenarios with cross barriers that induce transversal spreading of contaminant pathlines have negative trends in relative savings. Compared to the relative savings though, further inspection of the results revealed that, except for scenario down, the absolute difference in $\overline{Q}'$ between CPT and BPT generally increases with α ($\alpha > 10°$, Table 1).

Raising the variance of the transmissivity distribution, σ_Y^2, affects especially the relative $\overline{Q}'$ savings for the scenarios up and side as these become nearly insensitive to the gradient direction (Figure 9b). Barriers at the sides turn out to be especially beneficial due to their lateral blocking. The scenario side leads consistently to >25% relative savings in $\overline{Q}'$, which do not change remarkably for higher integral scales. Figure 9c denotes only minor changes for all BPT scenarios when increasing I_Y toward w. However, since the scenario-specific values of $\overline{Q}'$ generally rise with I_Y, the absolute savings also rise (Table 1). Savings by BPT are curbed by increasing the well distance x (Figure 9d). They are also less sensitive to changes in the gradient direction, denoting a fading role of barriers if x becomes large.

Of major interest are not only the mean savings in Q' but also the question whether barriers may also lead to unintentional higher pumping rates than required with CPT. The probability of occurrence of such a situation

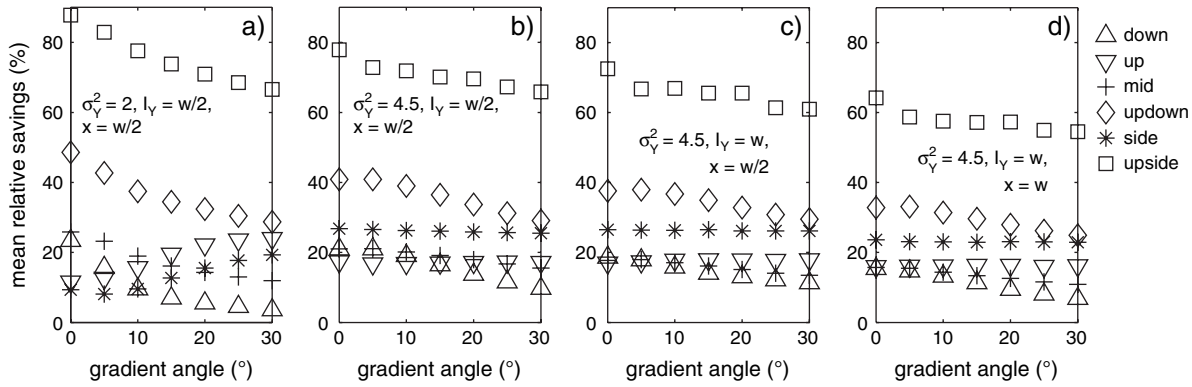

Figure 9. Mean relative savings in average pumping rate $\overline{Q}'$ for BPT scenarios compared to results for CPT for different settings of variance σ_Y^2, integral scale I_Y, and well distance x.

was evaluated for the same model parameter settings used before. To deduce the frequency of deteriorated results, the values of Q' for CPT and BPT scenarios have been compared for each individual realization during the Monte Carlo analysis. A striking feature of the results (Figure 10) is that commonly <2.5 % of the realizations gave worse results for nearly all BPT variants. Especially for low values of σ_Y^2, the percentage deterioration was close to zero. The downgradient barrier represents an outlier. The probability of higher Q' values increases from 5% to nearly 30% when raising the gradient incline. Obviously, this is due to the transversal spreading of the contaminant flow, which in several cases affords higher pumping rates than without the barrier. Also, the mid-position causes a lateral spreading and thus leads to slightly increasing deterioration frequencies. Figures 10a through 10d denote that the different model parameter settings have only a minor impact on the reliability of BPT and do not lead to a clear trend. However, though not shown here, at lower values of σ_Y^2 (<2), the percentage deterioration significantly decreases. This observation can again be attributed to a change from predominantly channeled to more distributed flow, thus decreasing the risk of contaminant flow strongly deflected from the pumping well.

In a further examination, the validity of the results obtained by 500 realizations was reassessed by comparing average pumping rates and calculations of savings to those obtained by alternative ensembles with the same statistics. For settings $I_Y/w = 0.5$ and 1.0 and $\sigma_Y^2 = 0.1$, 2.0, and 4.5, additional ensembles with 500 new realizations were created, yielding 1000 realizations in total for each given distribution. Oriented at Goovaerts' (1999) approach, 100 subsets of 500 realizations each were sampled randomly from the new ensemble without replacement. Minimum pumping rate calculations for scenarios CPT, down, side, and updown were then exemplarily inspected, assuming the distance of the well $x = w/2$. The standard deviations of $\overline{Q}'$over all subsets were <5%. We also examined if the calculated percentage of deterioration by barrier installation can be reproduced. Very good agreement with the results shown in Figure 10 was found for nearly all BPT scenarios. Even for the down scenario with an expected deterioration scoring >20%, the absolute standard deviation did not reach values >3%.

Table 1
Influence of Increases in Parameter Values on Absolute Savings in $\overline{Q}'$ of BPT Scenarios Compared to $\overline{Q}'$ of CPT

	Down	Up	Mid	Updown	Side	Upside
σ_Y^2 ($\alpha < 10°$)	+	+	+	+	+	+
σ_Y^2 ($\alpha > 10°$)	+	0	+	+	+	+
I_Y	+	+	+	+	+	+
x	−	−	−	−	−	−
α (<10°)	−	0	−	−	−	−
α (>10°)	−	+	+	+	+	+
b	+	+	+	+	+	+

+, positive; −, negative; 0, neutral trend.

Summary and Outlook

In this paper, we analyzed BPT for their effectiveness in controlling contaminant plumes in ground water. The focus was put on the discussion of the significance of deviations in the flow direction from a given and expected direction and to the consideration of highly heterogeneous aquifer conditions. Using a hypothetical contamination scenario, the performance of BPT was assessed in terms of the pumping rate required to completely capture a given contaminated area.

The presented work supports the findings from a preceding study (Bayer et al. 2004), providing clear evidence of the effectiveness and the robustness of BPT compared to CPT. The results of the presented paper specifically show that (1) BPT clearly outmatch CPT even if background ground water flow direction has been anticipated incorrectly; (2) BPT may yield considerable savings of up to 80% with respect to the expected value of required pumping rate compared to CPT; and (3) the risk that additional barriers will lead to an unwanted negative effect, i.e., higher pumping rates, is small (<2.5% for most of the proposed BPT scenarios).

Taking both the presented and the preceding investigation (Bayer et al. 2004) together, the potential benefits of BPT are now reliably confirmed, addressing major

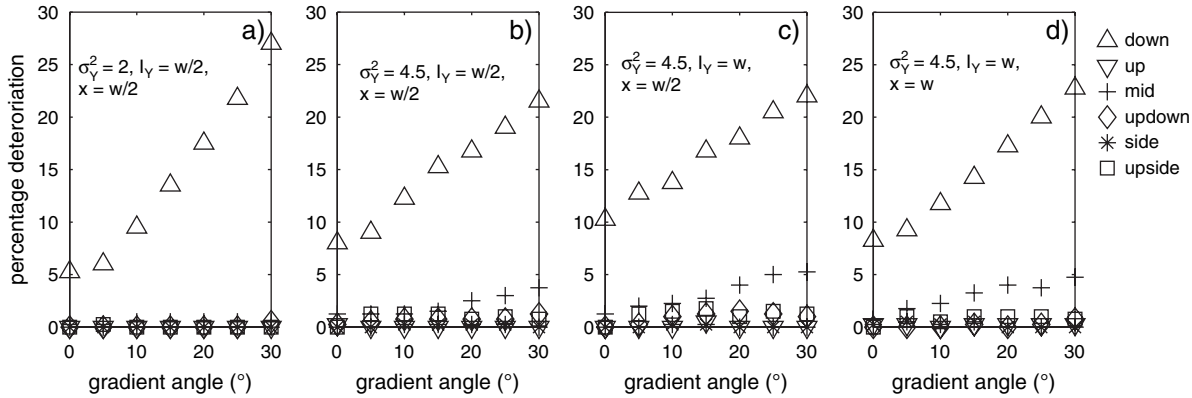

Figure 10. Percentage of increase in Q' for BPT scenarios compared to results for CPT based on Monte Carlo analysis.

factors of uncertainty that are known to potentially have a substantial impact on the success of hydraulic measures in ground water. It is discussed that the positive effect of vertical physical barriers can be especially attributed to the blocking of high permeability structures, i.e., preferred pathways, thereby retaining ground water flow previously focused to these structures and thus reducing required pumping rates. Since spatial variability of transmissivity has been considered by SGS, which does not preserve the occurrence of continuous structures (Gomez-Hernandez and Wen 1998), we may expect an even higher benefit of vertical physical barriers for spatial variability models, which have the potential to replicate continuity in preferential flowpaths, such as indicator simulation approaches. The relative importance of the choice of the spatial variability model, therefore, will be subject to further research. In this context, the role of existing conditioning field data gathered during site investigation will also have to be examined. Such data are likely to reduce parameter uncertainty, thus narrowing the variability of the results from Monte Carlo simulations. Aside from this, the existence of even sparse information on local transmissivity will involve a system optimization step leading to nonsymmetrical barrier settings that are adapted to the given site-specific characteristics as far as they can be determined from available information. The system optimization will have to cover both the positioning of the barriers and the pumping well or even a group of pumping wells (Bayer and Finkel 2004).

To deal with the above-mentioned issues, the focus has to be extended toward real world case studies and more close-to-reality scenarios. Based on these, the general validity and transferability of the findings from the generic modeling study presented can be examined in detail. Of particular interest are the roles of three-dimensional aquifer representations, partially penetrating wells, and typical hydraulic constraints like the limitation of ground water level changes from drawdown and backwater.

Acknowledgments

Financial support from the German Research Foundation (Deutsche Forschungsgesellschaft) for this project is gratefully acknowledged. Appreciation is also extended to the reviewers Doug Walker, Dirk Schulze-Makuch, and Frans van Geer for their careful attention. Their efforts have greatly improved this contribution.

References

Bair, E.S., C.M. Safreed, and E.A. Stasny. 1991. A Monte Carlo-based approach for determining traveltime-related capture zones of wells using convex hulls as confidence regions. *Ground Water* 29, no. 6: 849–855.

Bayer, P., and M. Finkel. 2004. Evolutionary algorithms for the optimization of advective control of contaminated aquifer zones. *Water Resources Research* 40, no. 6: W06506.

Bayer, P., M. Finkel, and G. Teutsch. 2005. Cost-optimal contaminant plume management with a combination of pump-and-treat and physical barrier systems. *Ground Water Monitoring and Remediation* 25, no. 2: 96–106.

Bayer, P., M. Finkel, and G. Teutsch. 2004. Hydraulic performance of a combination of pump-and-treat and physical barrier systems for contaminant plume management. *Ground Water* 42, no. 6: 856–867.

Bayer, P., M. Finkel, and G. Teutsch. 2003a. Bridging the gap between conventional pump-and-treat systems and permeable walls: Hydraulic and economic aspects of barrier-supported pump-and-treat systems. In: *CD Proceedings of the 8th International FZK/TNO Conference on Contaminated Soil (CONSOIL)*, Gent, Belgium, May 12–16, 2003, 1592–1600.

Bayer, P., M. Finkel, and G. Teutsch. 2003b. Reliability of hydraulic performance and cost-estimates of barrier-supported pump-and-treat systems in heterogeneous aquifers. In: *Calibration and Reliability in Groundwater Modelling: A Few Steps Closer to Reality*, ed. K. Kovar and Z. Hrkal, 331–338. IAHS Publication no. 277.

Bayer, P., M. Morio, C. Bürger, B. Seif, M. Finkel, and G. Teutsch. 2001. Funnel-and-gate vs. innovative pump-and-treat systems: A comparative economical assessment. In *Groundwater Quality: Natural and Enhanced Restoration of Groundwater Pollution*, ed. S.F. Thornton and S. Oswald, 235–244. IAHS Publication no. 275, Wallingford, U.K.

Carle, S.F., and G.E. Fogg. 1996. Transition probability based indicator geostatistics. *Mathematical Geology* 28, no. 4: 453–477.

Cole, B., and S. Silliman. 1997. Capture zones for passive wells in heterogeneous unconfined aquifers. *Ground Water* 35, no. 1: 92–98.

Cunningham, J.A., and M. Reinhard. 2002. Injection-extraction treatment well pairs: An alternative to permeable reactive barriers. *Ground Water* 40, no. 6: 599–607.

Deutsch, C.V., and A.G. Journel. 1992. *GSLIB: Geostatistical Software Library and User's Guide*. New York: Oxford University Press.

Erskine, A.D. 1991. The effect of tidal fluctuation on coastal aquifer in the UK. *Ground Water* 29, no. 4: 556–562.

Festger, A.D., and G.R. Walter. 2002. The capture efficiency map: The capture zone under time-varying flow. *Ground Water* 40, no. 6: 619–628.

Feyen, L., A.M. Dessalegn, F. De Smedt, S. Gebremeskel, and O. Batelaan. 2004. Application of a Bayesian approach to stochastic delineation of capture zones. *Ground Water* 42, no. 4: 542–551.

Gomez-Hernandez, J., and X.H. Wen. 1998. To be or not to be multi-Gaussian? A reflection on stochastic hydrogeology. *Advances in Water Resources* 21, no. 1: 47–61.

Goovaerts, P. 1999. Impact of the simulation algorithm, magnitude of ergodic fluctuations and number of realizations on the spaces of uncertainty of flow properties. *Stochastic Environmental Research and Risk Assessment* 13, no. 3: 161–182.

Gotway, C.A., and B.M. Rutherford. 1994. Stochastic simulation for imaging spatial uncertainty: Comparison and evaluation of available algorithms. In *Geostatistical Simulations*, ed. M. Armstrong and P.A. Dowd, pp. 1–16. Dordrecht, The Netherlands: Kluwer Academic Publishers.

Jacobson, E., R. Andricevic, and J. Morrice. 2002. Probabilistic capture zone delineation based on an analytic solution. *Ground Water* 40, no. 1: 85–95.

Leeuwen van, M., A.P. Butler, C.B.M. te Stroet, and J.A. Tompkins. 2000. Stochastic determination of well capture zones conditioned on regular grids of transmissivity measurements. *Water Resources Research* 36, no. 4: 949–957.

McDonald, M.G., and A.W. Harbaugh. 1988. A modular three-dimensional, finite difference ground-water flow model. In *U.S. Geological Survey Techniques of Water Resources Investigations*, book 6, chap. A1. Washington, DC. USGS.

Molz, F.J., H. Rajaram, and S. Lu. 2004. Stochastic fractal-based models of heterogeneity in subsurface hydrology: Origins, applications, limitations, and future research questions. *Reviews of Geophysics* 42.

Neuman, S.P., and V. Di Federico. 2003. Multifaceted nature of hydrogeologic scaling and its interpretation. *Reviews of Geophysics* 41, no. 3: 1014.

Pollock, D.W. 1994. User's guide for MODPATH/MODPATH-PLOT, version 3: A particle tracking post-processing package for MODFLOW, the U.S. Geological Survey finite-difference ground-water flow model. USGS Open-File Report 94–464. USGS.

Powell R.M., P.D. Powell, and R.W. Puls. 2002. Economic analysis of the implementation of permeable reactive barriers for remediation of contaminated ground water. EPA 600-R-02–034. Cincinnati, Ohio: U.S. EPA.

Pranzetti, S., and A. Guadagnini. 1996. Probabilistic estimation of well catchments in heterogeneous aquifers. *Journal of Hydrology* 174, no. 1–2: 149–171.

Press, W.H., B.P. Flannery, S.A. Teukolsky, and W.T. Vetterling. 1992. *Numerical Recipes in Fortran—The Art of Scientific Computing*, 2nd ed. Cambridge, U.K.: Cambridge University Press.

Reilly, T.E., and D.W. Pollock. 1996. Sources for water to wells for transient cyclic systems. *Ground Water* 34, no. 6: 979–988.

Schulze-Makuch, D., D.A. Carlson, D.S. Cherkauer, and P. Malik. 1999. Scale dependency of hydraulic conductivity in heterogeneous media. *Ground Water* 37, no. 6: 904–919.

Serfes, M.E. 1991. Determining the mean hydraulic gradient of groundwater effected by tidal fluctuations. *Ground Water* 29, no. 4: 549–555.

U.S. EPA. 2003. The DNAPL remediation challenge: Is there a case for source depletion? EPA/600/R–03/143. Cincinnati, Ohio: U.S. EPA.

Wen, X.H., and J. Gomez-Hernandez. 1998. Numerical modeling of macrodispersion in heterogeneous media: A comparison of multi-Gaussian and non-multi-Gaussian models. *Journal of Contaminant Hydrology* 30, no. 1–2: 129–156.

Zawadzki W., D.W.Chorley, and G. Patrick. 2002. Capture-zone design in an aquifer influenced by cyclic fluctuations in hydraulic gradients. *Hydrogeology Journal* 10, no. 6: 601–609.

Zhang, D.X., and Z.M. Lu. 2004. Stochastic delineation of well capture zones. *Stochastic Environmental Research* 18, no. 1: 39–46.

Zinn B., and C.F. Harvey. 2003. When good statistical models of aquifer heterogeneity go bad: A comparison of flow, dispersion, and mass transfer in connected and multivariate Gaussian hydraulic conductivity fields. *Water Resources Research* 39, no. 3: 1051.